Electrostatic and Hydrophobic Interactions Involved in CNT Biofunctionalization with Short ss-DNA

ARTICLE *in* THE JOURNAL OF PHYSICAL CHEMISTRY C · MARCH 2010

Impact Factor: 4.77 · DOI: 10.1021/jp9085359 · Source: PubMed

Published in final edited form as:
J Phys Chem C Nanomater Interfaces. 2010 March 18; 114(10): 4459–4465. doi:10.1021/jp9085359.

Electrostatic and hydrophobic interactions involved in CNT biofunctionalization with short ss-DNA

Maria Lucrecia Carot,
INFIQC. Departamento de Fisicoquímica. Facultad de Ciencias Químicas. Universidad Nacional de Córdoba. (5000) Córdoba. Argentina

Roberto M. Torresi,
Instituto de Química. Universidade de São Paulo.CP 26077 - 05513-970. São Paulo. Brazil

Carlos D. Garcia,
Department of Chemistry. The University of Texas at San Antonio. One UTSA Circle. San Antonio. TX 78249. USA

Maria Jose Esplandiu, and
Grup de Sensors i Biosensors. Departament de Química. Universitat Autònoma de Barcelona. Edifici C. Campus de la UAB. 08193. Bellaterra. Cerdanyola del Vallés. Barcelona. Spain

Carla E. Giacomelli[*]
INFIQC. Departamento de Fisicoquímica. Facultad de Ciencias Químicas. Universidad Nacional de Córdoba. (5000) Córdoba. Argentina

Abstract

This work is aimed at studying the adsorption mechanism of short chain 20-mer pyrimidinic homo-ss-DNA (oligodeoxyribonucleotide, ODN: polyC_{20} and polyT_{20}) onto CNT by reflectometry. To analyze the experimental data, the effective-medium theory using the Bruggemann approximation represents a suitable optical model to account for the surface properties (roughness, thickness and optical constants) and the size of the adsorbate. Systematic information about the involved interactions is obtained by changing the physico-chemical properties of the system. Hydrophobic and electrostatic interactions are evaluated by comparing the adsorption on hydrophobic CNT and on hydrophilic silica and by modulating the ionic strength with and without Mg^{2+}. The ODN adsorption process on CNT is driven by hydrophobic interactions only when the electrostatic repulsion is suppressed. The adsorption mode results in ODN molecules in a side-on orientation with the bases (non-polar region) towards the surface. This unfavorable orientation is partially reverse by adding Mg^{2+}. On the other hand, the adsorption on silica is dominated by the strong repulsive electrostatic interaction that is screened at high ionic strength or mediated by Mg^{2+}. The cation-mediated process induces the interaction of the phosphate backbone (polar region) with the surface, leaving the bases free for hybridization. Although the general adsorption behavior of the pyrimidine bases is the same, polyC_{20} presents higher affinity for the CNT surface due to its acid-base properties.

[*] To whom correspondence should be addressed. Phone: 54-351-4334169/54-351-4334180. Fax: 54-351-4334188. giacomel@fcq.unc.edu.ar.

Supporting Information Available. AFM image and profiles recorded for the Si/SiO_2 sorbent surface in aqueous solution, calculated effect of a) the adsorbed ODN conformation on the relative change in the reflectometry signal as a function of the surface coverage and b) the adsorbed amount on the change in the reflectometry signal. Detailed description on the calculation of the Q-factor. This material is available free of charge via the Internet at http://pubs.acs.org.

Keywords

Oligodeoxyribonucleotide; ODN; Adsorption; Solid Surfaces; Reflectometry

Introduction

Nucleic acid hybridization is widely used in the detection of the specific complementary strands in molecular biology and applied fields, such as diagnostic in medicine. An ideal system for these applications results when solid surfaces are combined with short single-stranded oligodeoxyribonucleotide (ODN), a fragment of ss-DNA, to induce surface hybridization with the complementary strand present in solution. Among the different possibilities of sorbent surfaces, carbon nanotubes (CNTs) exhibit interesting structural, mechanical, electrical and electromechanical properties to be combined with the biological recognition capabilities for applications in bioengineering, clinical medicine, and bionanotechnology[1-5].

Surface biofunctionalization to develop DNA-platforms for hybridization detection relies on covalent bond formation or simple adsorption of short ODN. Covalent interaction has been achieved with thiolated ODN on gold surfaces[6-8] and nanoparticles[6,9] and CNTs[10-12] while physical interaction has been studied on graphite[13-15] and silica[16-18] surfaces, polystyrene particles[19-23], and liposomes[24]. Clearly, irrespective of the strategy used to induce the surface-ODN interaction, the capability of hybridization in such a system is controlled by the orientation and conformation of the adsorbed ODN molecules, which depend on the ODN sequence, the surface properties and the solution conditions. It is commonly reported that both electrostatic and hydrophobic interactions are major driving forces for ODN adsorption at solid-liquid interfaces[16,18]. The general adsorption behavior of ODN is described by a higher affinity of the purine bases (guanine and adenine) than the pirymidine ones for the surface (such as graphite and gold) following their hydrophobic scale[8,9,14,15,25]. The pH and ionic strength of the solution mainly affects the structure and flexibility of ODN molecules: higher adsorbed amounts are reported for less rigid conformations[8,9,14,15,26]. However, relatively little is known about the adsorption mechanism, the adsorbed amount in steady state and the effect of these interactions on the interfacial behavior of single-stranded ODN molecules[16,22].

The purpose of the present work is to study the adsorption mechanism of synthetic single-stranded homo-ODN onto CNT coated silica surfaces by reflectometry. In view of the practical application, this study is especially focused on how this process is affected by the interactions between ODN molecules and the sorbent and on how these biomolecule-surface interactions determine the orientation of the adsorbed ODN molecules. Systematic information about the involved interactions is obtained by changing the physico-chemical properties of the system. Hydrophobic interactions are evaluated by comparing the adsorption on hydrophobic CNT and on hydrophilic silica. The electrostatic interactions are tested by modulating the ionic strength (IS = 0.001, 0.1, 0.2) with and without Mg^{2+} cations. Further, the effect of the bases on the adsorption process is analyzed with short chain 20-mer pyrimidinic homo-ODN (polyC_{20} and polyT_{20}).

Reflectometry enables a continuous monitoring of the adsorbed amount in real time, from the first contact up to reaching steady state conditions. Although this optical technique has been widely applied to study the adsorption-desorption process of proteins[27-29] and polymers[30] on different flat, homogeneous surfaces, it has not been used with small polyelectrolytes (short ODN) and rough surfaces (CNT coated silica). Therefore, a suitable optical model considering the surface properties, such as roughness, thickness and optical

constants, and the size of the adsorbate is presented to properly analyze the experimental data.

Experimental Section

Chemical and Instrumentation

The 20-mer polycytosine and polythymine ($PolyC_{20}$ and $PolyT_{20}$) were purchased from Integrated DNA Technologies, Inc. (1710 Commercial Park Coralville, IA 52241) and Invitrogen Corporation. Aqueous solutions were prepared in 18 MΩ/cm resistance water (Milli-Q, Millipore; Billerica, MA) using analytical grade reagents (without further purification): NaH_2PO_4, NaCl and $MgCl_2$ (Baker). Phosphate buffer (PB) was prepared by dissolving the desired amount of NaH_2PO_4 (Baker) in water and adjusting the pH with either 2 M NaOH or 2 M HCl (Baker). The pH measurements were performed with a combined glass electrode and a digital pH meter (Orion 420A, Thermo; Waltham, MA). Unless otherwise noted, all experiments were performed at room temperature (22 ± 2 °C).

Substrates

Either silica (Si/SiO_2) or CNT-coated silica (Si/SiO_2/CNT) surfaces were used for the adsorption experiments. In the former case, silicon wafers (100 mm, Silicon Valley Microelectronics Inc.; Santa Clara, CA) were oxidized for 1 h at 1000 °C in order to obtain a silica layer of approximately 100 nm thick, which was verified by ellipsometry. Such a thickness is essential for obtaining a high sensitivity in reflectometry experiments[31]. The wafer was then cut in strips (1 cm × 3 cm) following the crystallographic plane. Prior to each experiment, the silica strips were cleaned with boiling piranha solution (2:1 H_2SO_4:H_2O_2) and rinsed thoroughly with deionized water. *(Caution! Piranha solution is a powerful oxidizing agent that reacts violently with organic compounds; it should be handled with extreme care).*

As described in earlier studies[27,32], Si/SiO_2/CNT surfaces were prepared by Eikos Inc. (Franklin, MA), using (111) silicon/ SiO_2 wafers (Sumco, Phoenix, AZ, d_{SiO2} = 2 nm) as substrates. According to the provider, a layer of CNT was deposited on the wafers using arc-produced single-wall CNT having about a 1.3 nm diameter. The raw material formed in the arc reactor was purified, to remove metal catalyst and non-tubular forms of carbon, by a process of acid reflux, followed by washing and centrifugation. Once purified, the nanotubes were dispersed in water and alcohol to form an ink. This dispersion was then spray-coated onto the Si/SiO_2 wafer heated to 65 °C while monitoring deposition rate. The coating formed is essentially a layer of pure CNT and contains no residual organic additives or polymeric constituents.

Atomic Force Microscopy (AFM)

Topographic images were obtained using a PicoSPM-LE Molecular Imaging system (Tempe, AZ) in aqueous solution with cantilevers operating in the intermittent-contact mode (MAC mode), slightly below their resonance frequency of approximately 290 KHz. All topographic images represent unfiltered original data and refer to scan areas of 4 μm × 4 μm. At least two samples of the same material were analyzed at different areas of the surface. At least 90 profiles obtained from the AFM images were analyzed to characterize these surfaces.

Image processing and roughness determination (R_a) were performed by using PicoScan 5.4 (Molecular Imaging Corporation).

Reflectometry

Adsorption-desorption measurements were performed in a reflectometer (AKZO Research Laboratories, Arnhem), using a stagnation point flow cell as described by Dijt et al.[31,33]. This measurement is based on the change of surface reflectivity (R, the ratio between the intensities of the parallel (p) and perpendicular (s) components of the reflected light) during the adsorption process. In a typical reflectometer experiment, the relative signal change ($\Delta S/S_0$) is recorded as a function of time upon macromolecule addition:

$$\frac{\Delta S}{S_0}=\left[\frac{\left(\frac{R_p}{R_s}\right)_\Gamma-\left(\frac{R_p}{R_s}\right)_0}{\left(\frac{R_p}{R_s}\right)_0}\right]=\frac{\Delta R}{R_0} \quad (1)$$

where the subscripts "Γ" and "0" indicate the presence of an adsorbed layer and the initial state of a bare surface, respectively. Therefore, during the measurement $\Delta S/S_0$ or $\Delta R/R_0$ changes from zero in the presence of background electrolyte to a given positive value due to the adsorption.

Using the appropriate experimental setup (incident angle, sorbent refractive index, adsorbed amount, etc.), $\Delta S/S_0$ is proportional to the adsorbed amount (Γ)[31,33]:

$$\Gamma=Q\frac{\Delta S}{S_0} \quad (2)$$

The Q-factor is calculated by considering the surface properties, such as roughness, thickness and optical constants (refractive index and absorption coefficient) before and after adsorption (see supplementary information). Therefore, to determine Γ from $\Delta S/S0$ it is necessary to develop an appropriate surface model to account for all these parameters. In this regard, reflectometry data are treated in the same way as ellipsometry ($R = R_p/R_s = \tan(\psi)\, e^{i\Delta}$) data from which an optical model is also needed to calculate Γ from ψ and Δ[33,34].

On the other hand, one of the main advantages of the reflectometer setup is that the transport of macromolecules towards the surface is well controlled by a stagnation point flow[31,33]. The hydrodynamic of the mass flux in a stagnation point flow was previously described in detail[33,35]. In the absence of an adsorption barrier, the initial limiting flux J_0 (mg m^2 /s) towards the surface is described by the following equation,[31,33]:

$$J_0=0.53\left(D^2\alpha\phi R^{-4}\right)^{1/3}C_{ODN}=kC_{ODN} \quad (3)$$

where D is the diffusion coefficient of ODN (3×10^{-8} m^2 s^{-1} [26]), α a dimensionless flow intensity parameter which is constant for a given cell geometry and flow rate (3.5), ϕ the flow rate (2.5×10^{-8} m^3 s^{-1}), R the radius of the circular hole through which the solution enters the cell (0.9×10^{-3} m) and C_{ODN} the ODN concentration in mg m^{-3}. The calculated value for k is 4.9×10^{-4} m s^{-1}.

Ellipsometry

The substrate characterization was performed at room temperature using a variable angle spectroscopic ellipsometer (VASE, J. A. Woollam Co.; Lincoln, NE). Spectroscopic ellipsometry provides useful information about the optical constants and structure of the adsorbed film[36]. Substrates were analyzed in air and water, using light reflection p-polarization and s-polarization by varying the angle of incidence. Ellipsometry data (amplitude ratio (Ψ) and phase difference (Δ) as a function of wavelength were obtained using the WVASE® software package. The sample under investigation was mounted on a micrometer-position-controlled translation stage with the gradient direction perpendicular to the plane of incidence. Substrates were characterized in air and water, varying the incident angle between 60° and 70° (with respect to the substrate) and the wavelength between 250 and 900 nm.

Results and Discussion

Surface Characterization

The topography and roughness profiles of CNT covered Si/SiO_2 wafers are shown in Figure 1. The presence of CNT strongly changes the surface topography, from a surface roughness of 0.6 ± 0.1 nm (bare Si/SiO_2, see supplementary information) to 6 ± 1 nm (CNT covered Si/SiO_2). The AFM image and profiles show that the bare Si/SiO_2 is rather flat with an oxide layer of 80 ± 5 nm (as determined by ellipsometry). On the other hand, the CNT-coated silica wafers are a randomly distributed network of SWCNT bundles with a high proportion of void space. The AFM roughness profiles show that the thickness of the CNT film is 35 ± 13 nm, which is in very good agreement with the ellipsometry results reported in the literature[27,32]. Based on these results, it follows that the optical model needed to calculate Γ from $\Delta S/S_0$ (eq. (2)) depends on the sorbent surface.

Reflectometry and ellipsometry are indirect methods because the measured $\Delta S/S_0$, or ψ and Δ are not converted directly into the surface properties (refractive index, thickness, adsorbed amount, etc) of the sample. Consequently, an optical model that describes the surface microstructure in terms of the complex refractive index (N = n - *i*k), and thickness (d) is required to interpret either $\Delta S/S_0$ or ψ and Δ experimental data. Usually, the optical model is applied by analyzing the Fresnel reflectivities for a stratified system of uniaxial layers with optical axes parallel to the substrate surface[27]. On these bases, the reflectivity of the Si/SiO_2 wafer is determined by the interference of the light reflected at two boundaries: aqueous solution/ SiO_2 and SiO_2/Si. Therefore, these substrates were modeled as a semi-finite layer of Si (N_{Si} = 3.80 - *i*0.02), a SiO_2 layer (N_{SiO2} = 1.46 - *i*0.00 and d_{SiO2} = 80 ± 5 nm), and the semi-finite bulk solution (N_{H2O} = 1.33 - *i*0.00). On the other hand, the reflectivity of the CNT-coated silica wafer is determined by three interfaces: aqueous solution/CNT, CNT/ SiO_2 and SiO_2/Si. The SiO_2 and Si complex refractive indices are the same as used in the former case, with a thinner oxide layer (d_{SiO2} = 2 nm). The microscopic roughness of the CNT layer was accounted for by applying the effective-medium theory (EMT) using the Bruggemann approximation[37,38]. In this approach, the rough surface is treated as a single layer of two components: the aqueous solution and the CNTs. This layer has effective thickness and optical constants, which result from the combination of the optical constants of the two components. In order to compute the effective optical constants of the CNT layer, both $\Delta S/S_0$ (reflectometry) and ψ and Δ (ellipsometry) were determined in air and in water. The experimental R_p and R_s data were fit by adjusting only the effective complex refractive index of the CNT layer using the thickness determined by AFM (d_{CNT} = 35 ± 13 nm) as an input parameter. This calculation gives N_{CNT} = 1.38 ± 0.01- *i* (0.013 ± 0.009) in good agreement with reported results[32,39].

Odn Adsorption

Figure 2A shows a typical reflectometry experiment, where the relative change of the signal ($\Delta S/S_0$) was followed as a function of time, to monitor the adsorption-desorption process of polyC_{20} on Si/SiO_2/CNT. Initially (from 0 to 200 s), only the buffer solution (5 mM PB + 100 mM NaCl, pH 7) was introduced in the cell to record a stable baseline. Then (from 200 to 1600 s), the flow was switched from buffer to a 13 μg/mL polyC_{20} solution (prepared in the same buffer). A significant increase in the signal is observed as a consequence of the adsorption of polyC_{20} on the surface. Next (between 1600 to 2200 s), the flow was switched back to the initial buffer solution in order to measure desorption upon dilution.

To calculate the adsorbed amount on flat surfaces from the reflectometry data, the concentration profile described by Dijt[31,33] is usually adopted. In this model, adsorbed ODN is treated as an inhomogeneous layer characterized by its complex refractive index (n_{ODN}; $k_{ODN} = 0$) with an adsorbed amount Γ of average thickness d_{ODN}:

$$n_{ODN} = n_s + \left(\frac{d_n}{dC}\right)_{ODN} \frac{\Gamma}{d_{ODN}} \quad (4)$$

where n_s is the refractive index of the aqueous solution, $(d_n/dC)_{ODN}$ is the refractive index increment (specific refractivity) of the adsorbed biomolecule layer and Γ/d_{ODN} is the concentration in the adsorbed biomolecule layer. On the other hand, when small ODN molecules adsorb on the rough CNT surface two adsorption modes may be possible: monolayer adsorption or surface aggregation. In the first case, n_{ODN} is calculated from eq. 4 while to account for surface aggregation, the Bruggemann approximation is used with three components (aqueous solution, ODN and CNT). The dependence of $\Delta S/S_0$ with surface coverage (see supplementary information) shows that surface aggregation causes a signal change as high as 0.1 at low surface coverage (θ = 0.2), whereas side-on adsorption results in signal changes compatible with the experimental data. Therefore, eq. 4 was also used to compute the adsorbed amount on CNT. The *Q*-factor was calculated (see supplementary information) assuming ODN adsorption in a side-on orientation with a thickness of the ODN layer (d_{ODN}) close to the ODN dimensions (20 × 3.4 Å length × 10 Å radius[16]). It is worth noting that d_{ODN} is not critical because the *Q*-factor (eq. (2)) is almost insensitive to its actual value[31,33]. A value of 0.153 $cm^3\ g^{-1}$ [40] was assumed for the specific refractivity of the ODN layer and considered constant at all surface concentrations. The calculated *Q*-factors were 32 ± 2 mg m^{-2} for Si/SiO_2 and 8 ± 3 mg m^{-2} for Si/SiO_2/CNT. The *Q*-factor standard deviation is mainly due to the thickness deviation of the SiO_2 layer (80 ± 5 nm) in the first case and to the CNT film (35 ± 13 nm) in the later one.

Figure 2B presents the adsorbed amount (Γ), as calculated from the $\Delta S/S_0$ values shown in Figure 2A, of polyC_{20} on Si/SiO_2/CNT as a function of time using the average *Q*-factor value (8) and this value plus (11) and minus (5) the standard deviation. Considering that the experimental measurements are performed with approximately 1 mm^2 laser spot, the average *Q*-factor was used to calculate all the informed Γ values. Quantitative determination of Γ from the reflectometry data implies that the *Q*-factor is constant, independent of Γ, i.e. the relationship between R_p/R_s and Γ is linear[31,33]. This linearity is kept up to 4 mg m^{-2} with a small deviation (20%) at 10 mg m^{-2} (see supplementary information). This analysis also allows determining that the reflectivity ratio R_p/R_s changes about 10% per mg m^{-2} adsorbed, indicating that an amount as low as (4 μg m^{-2}) is, in principle, detectable. However, when the $\Delta S/S_0$ is as low as the experimental values obtained when polyC_{20} adsorbs on either CNT or silica, the uncertainty given by two independent measurements is around 25 %.

Figure 3 shows the adsorption isotherm of $polyC_{20}$ on CNT surface at pH 7 in PB + 100 mM NaCl as obtained from the saturation adsorbed amounts (measured at steady state from curves as the one shown in Figure 2B) as a function of ODN concentration. The magnitude of the error bars was calculated from the uncertainty given by two independent measurements. Adsorption of $polyC_{20}$ on CNT only takes place when 100 mM NaCl was added to the buffer (ionic strength = 0.11), whereas there is no adsorption on Si/SiO_2 surface at pH 7 neither at low (without NaCl) nor at high (100 mM NaCl) ionic strengths. The maximum adsorbed amount (200 ± 50 μg m^{-2}) measured on CNT is in agreement with the value informed in the literature for hydrophobic surfaces, and for the hydrophobic contribution to the adsorption on positively charged surfaces[20,21,41]. Moreover, on partially aminated silica surfaces the ODN adsorbed amount only reaches 20% of this value[16].

Oligonucleotides are strong polyelectrolyte carrying a univalent negative charge per base at pH>2 containing nitrogenous bases that are hydrophobic in nature. The combination of the ionic and hydrophobic character results in complex adsorption behavior on solid surfaces. Silica is a hydrophilic negatively charged sorbent surface at pH 7[16,42]. Therefore, the strong repulsive electrostatic force between the hydrophilic silica and $polyC_{20}$ dominates their interaction and no adsorption is observed. The CNT sorbent is hydrophobic with carboxylate groups, produced during the purification by acid reflux, which provide negative charges to the surface[5,43]. $PolyC_{20}$ is only adsorbed on the hydrophobic CNT surface when the electrostatic repulsion is screened by adding sodium chloride. At relatively high salt concentrations, electrostatic effects are suppressed and the hydrophobic interaction between the non-polar region of the ODN molecules and the hydrophobic surface dominates, favoring the adsorption[4,44-46]. Therefore, $polyC_{20}$ adsorbs with the bases towards the CNT surface adopting an unfavorable orientation for hybridization, demonstrating that to properly biofunctionalize the surface, hydrophobic interactions need to be minimized.

The adsorption mode of $polyC_{20}$ with the bases towards the CNT surface agrees with the proposed adsorption mode of ODN molecules in a side-on orientation used to calculate the *Q*-factor. Furthermore, nucleic acid single strands keep a rigid structure resembling the base-paired double-strand helical conformation and adopt a flat conformation in the adsorbed state with the long axis parallel to the surface[15,18,23,46]. The low maximum adsorbed amount experimentally observed may be due to the increasing electrostatic repulsion created as the ODN layer is built up. When a certain concentration is reached, this repulsive electrostatic contribution to the adsorption energy dominates over the attractive hydrophobic contribution and limits further ODN-surface interaction.

Figure 4 compares the adsorption–desorption kinetic curves (Γ vs. t) of $polyC_{20}$ and $polyT_{20}$ on CNT at the same pH (7) and ionic strength (PB + 100 mM NaCl, IS = 0.11). The magnitude of the error bars was calculated from the uncertainty given by two independent measurements. As it was the case with $polyC_{20}$, $polyT_{20}$ molecules do not adsorb on silica (with or without NaCl) and they only adsorb on CNT at an ionic strength of 0.11. The initial adsorption rates for both ODN are, within experimental error, of the same magnitude (1.8 ± 0.5 μg/m^2s and 1.6 ± 0.4 μg/m^2s for $polyC_{20}$ and $polyT_{20}$, respectively) indicating that the adsorption mechanism does not depend on the nature of the bases. Furthermore, these initial adsorption rates are lower than the mass flow (eq. (3)), highlighting the relevance of an electrostatic barrier (negative surface and ODN) that slows-down the adsorption process.

On the other hand, the adsorbed amount in the steady state and the percentage desorbed by dilution strongly depend on the nature of bases. The large difference in surface coverage between $polyC_{20}$ (200 ± 50 μg/m^2) and $polyT_{20}$ (50 ± 10 μg/m^2) are not related to hydrophobicity because the differences between them in molecular structure are very small[14]. However, the acid-base behavior of the nucleotides is rather different. At low pH,

cytosine base is positively charged due to the protonation of the amino group, whereas thymine is neutral. At high pH, cytosine base is neutral, whereas thymine is negatively charged due to the deprotonation of the amino group[42,47]. Therefore, the electrostatic interactions between polyT_{20} and CNT are more unfavorable than those of polyC_{20}, resulting in a lower affinity[25]. In line with this behavior, the desorbed percentage upon dilution is almost negligible (lower than 10%) for polyC_{20} while reaches 30% for polyT_{20}. This adsorption behavior is in agreement with the results reported for the pyrimidinic ODN adsorbed on gold at pH 7[8,9,25].

To minimize the hydrophobic interactions that promote an unfavorable orientation for hybridization, electrostatic repulsion was reduced by either increasing the ionic strength or adding divalent cations. Figure 5 shows the adsorption-desorption kinetics of polyT_{20} on (A) CNT and (B) silica sorbent surfaces at pH 7 and two ionic strengths (0.11 and 0.22) with and without adding Mg^{2+} ions. The initial adsorption rates, saturation adsorbed amounts and percentage desorbed upon dilution are given in Table 1. In the absence of divalent cations (open triangles), increasing the ionic strength up to 0.22 enables adsorption on silica surface. Furthermore, when comparing Figures 4 and 5 it follows that increasing the ionic strength strongly enhances the initial adsorption rate and the adsorbed amount on CNT. The general features of the adsorption-desorption curves are invariant with the sorbent surfaces and the desorbed percentage on CNT is independent of NaCl concentration. ODN molecules in solution become more flexible as the ionic strength increases[26] suggesting that they adopt a less rigid conformation on the surface. The screening of the electrostatic repulsion between the negatively charged phosphate groups increases the molecule flexibility, lowers the electrostatic adsorption barrier and improves the adsorbed amount. However, the desorbed percentage indicates that the interaction with the surface is of the same magnitude regardless the ODN flexibility suggesting that the adsorption mode does not depend on Na^{+} concentration.

When Mg^{+2} ions are present, the adsorption-desorption process depends on the sorbent surface (see Figure 5 and Table 1). On the hydrophilic silica, the presence of Mg^{2+} (higher than 10 mM) enhances the adsorption and increases the affinity of ODN for the surface. The desorbed percentage indicates that the interaction between polyT_{20} and silica becomes stronger as the Mg^{2+} concentration increases. As proposed for the interaction of ODN with other hydrophilic surfaces[17,24, 48-51], polyT_{20} adsorbs on Si/SiO_2 mediated by Mg^{2+} cations with the phosphate backbone towards the surface.

As shown in Figure 5 and Table 1, the adsorption-desorption process on the hydrophobic CNT further depends on the relative concentration of the divalent to monovalent ions. At 100 mM Na^{+}, the initial adsorption rate and the saturation adsorbed amount slightly increase with Mg^{2+} concentration. On the other hand, in the absence of Na^{+} (at the same ionic strength) both the initial adsorption rate and the saturation adsorbed amount are strongly affected by Mg^{2+}. Therefore, Na^{+} ions reduce ODN adsorption suggesting a competition between the cations involved in the polyT_{20} adsorption process. This competition may be due to the combination of hydrophobicity and negative charges on the CNT sorbent surface. Without divalent cations in 100 mM Na^{+}, the repulsion between the negative polyT_{20} and the surface is screened and the adsorption takes place by hydrophobic interactions. As described for Si/SiO_2, these experimental results suggest that Mg^{+2} is able to mediate ODN adsorption on CNT, improving the affinity with the surface. Consequently, the adsorption of polyT_{20} on CNT involves hydrophobic and Mg^{+2} mediated interactions, partially solving the unfavorable orientation caused by the bases facing the surface.

Conclusions

The rough CNT sorbent surface is properly described by applying the effective-medium theory using the Bruggemann approximation. The optical model describes the surface microstructure in terms of a combination between aqueous solution and CNTs with effective thickness and optical constants.

The adsorption process of short homo-ODN on the hydrophobic CNT surface is driven by hydrophobic interactions only when the electrostatic repulsion is suppressed. The adsorption mode results in ODN molecules in a side-on orientation with the bases (non-polar region) towards the surface. This unfavorable orientation is partially reverse by adding Mg^{2+}. On the other hand, the adsorption on the hydrophilic, negative silica is dominated by the strong repulsive electrostatic interaction that is screened at high ionic strength or mediated by Mg^{2+}. The cation mediated process induces the interaction of the phosphate backbone (polar region) with the surface, leaving the bases free for hybridization. Although the general adsorption behavior of the pyrimidine bases is the same, polyC_{20} presents higher affinity for the CNT surface due to its acid-base properties.

Supplementary Material

Refer to Web version on PubMed Central for supplementary material.

Acknowledgments

Authors acknowledge the financial contributions of FONCyT, SeCyT-UNC, CONICET, the International Exchange Collaboration between CAPES (Brazil) and SPU (Argentine) (Grant N° 025/05), and National Institute of General Medical Sciences (NIGMS)/National Institutes of Health (1SC3GM081085) (C. D. G). M. J. E. thanks the Ministry of Education and Science of Spain (Project NAN2004-093006-C05-03) and the “Ramón and Cajal” Program. M. L. C. thanks CONICET for the fellowship granted.

References

1. Valcárcel M, Cárdenas S, Simonet BM. Anal Chem 2007;79:4788–4797. [PubMed: 17542556]
2. Agüí L, Yáñez-Sedeño P, Pingarrón JM. Anal Chim Acta 2008;622:11–47. [PubMed: 18602533]
3. Cao C, Kim JH, Yoon D, Hwang E, Kim Y, Baik S. Mater Chem Phys 2008;112:738–741.
4. Meng L, Fu C, Lu Q. Prog Nat Sci 2009;19:801–810.
5. Wang J, Lin Y. Trends Anal Chem 2008;27:619–626.
6. Demers LM, Mirkin CA, Mucic RC, Reynolds RA, Letsinger RL, Elghanian R, Viswanadham G. Anal Chem 2000;72:5535–5541. [PubMed: 11101228]
7. Herne TM, Tarlov MJ. J Am Chem Soc 1997;119:8916–8920.
8. Demers LM, Östblom M, Zhang H, Jang N, Liedberg B, Mirkin CA. J Am Chem Soc 2002;124:11248–11249. [PubMed: 12236721]
9. Storhoff JJ, Elghanian R, Mirkin CA, Letsinger RL. Langmuir 2002;18:6666–6670.
10. Cai H, Cao X, Jiang Y, He P, Fang Y. Anal Bioanal Chem 2003;375:287–293. [PubMed: 12560975]
11. He P, Dai L. Chem Commun 2004:348–349.
12. Li J, Ng HT, Cassell A, Fan W, Chen H, Ye Q, Koehne J, Han J, Meyyappan M. Nano Lett 2003;3:597–602.
13. Manohar S, Mantz AR, Bancroft KE, Hui C, Jagota A, Vezenov DV. Nano Lett 2008;8:4365–4372. [PubMed: 19368004]
14. Chiorcea Paquim A, Oretskaya TS, Oliveira Brett AM. Biophys Chem 2006;121:131–141. [PubMed: 16460874]
15. Sowerby SJ, Cohn CA, Heckl WM, Holm NG. PNAS 2001;98:820–822. [PubMed: 11158553]

16. Balladur V, Theretz A, Mandrand B. J Colloid Interface Sci 1997;194:408–418. [PubMed: 9398423]
17. Cheng H, Zhang K, Libera JA, Olvera De La Cruz M, Bedzyk MJ. Biophys J 2006;90:1164–1174. [PubMed: 16449197]
18. Chan V, Mckenzie SE, Surrey S, Fortina P, Graves DJ. J Colloid Interface Sci 1998;203:197–207.
19. Walker HW, Grant SB. Langmuir 1995;11:3772–3777.
20. Ganachaud F, Elaïssari A, Pichot C. Langmuir 1997;13:7021–7029.
21. Elaïssari A, Pichot C, Delair T, Cros P, Kürfurst R. Langmuir 1995;11:1261–1267.
22. Walker HW, Grant SB. J Colloid Interface Sci 1996;179:552–560.
23. Ganachaud F, Elaïssari A, Pichot C, Laayoun A, Cros P. Langmuir 1997;13:701–707.
24. Patil SD, Rhodes DG. Nucleic Acids Res 2000;28:4125–4129. [PubMed: 11058108]
25. Kimura-suda H, Petrovykh DY, Tarlov MJ, Whitman LJ. J Am Chem Soc 2003;125:9014–9015. [PubMed: 15369348]
26. Murphy MC, Rasnik I, Cheng W, Lohman TM, Ha T. Biophys J 2004;86:2530–2537. [PubMed: 15041689]
27. Valenti LE, Fiorito PA, García CD, Giacomelli CE. J Colloid Interface Sci 2007;307:349–356. [PubMed: 17174970]
28. Riquelme BD, Valverde JR, Rasia RJ. Opt Laser Eng 2003;39:589–598.
29. Bosker WT, Iakovlev PA, Norde W, Cohen Stuart MA. J Colloid Interface Sci 2005;286:496–503. [PubMed: 15897063]
30. Stuart, MA.; de Keizer, A. Oxide Surfaces. Wingrave, J., editor. Marcel Dekker; New York: 2001. p. 157-199.
31. Dijt JC, Cohen Stuart MA, Fleer GJ. Adv Colloid Interface Sci 1994;50:79–101.
32. Barnes TM, van De Lagemaat J, Levi D, Rumbles G, Coutts TJ, Weeks CL, Britz DA, Levitsky I, Peltola J, Glatkowski P. Phys Rev B 2007;75:235410.
33. Dijt JC, Cohen Stuart MA, Hofman JE, Fleer GJ. Colloids Surf 1990;51:141–158.
34. Azzam, RM.; Bashara, NM. Ellipsometry and Polarized Light. North-Holland: 1977.
35. Atkin R, Craig VS, Wanless EJ, Biggs S. Adv Colloid Interface Sci 2003;103:219–304. [PubMed: 12781966]
36. Mora MF, Giacomelli CE, Garcia CD. Anal Chem 2009;81:1016–1022. [PubMed: 19132842]
37. Aspnes DE. J Mater Educ 1985;7:849.
38. Nee SF. Appl Optics 1988;27:2819–2831.
39. de Los Arcos T, Oelhafen P, Mathys D. Nanotechnology 2007;18:265706.
40. McLoughlin D, Langevin D. Colloids Surf A 2004;250:79–87.
41. Elaïssari A, Chauvet JP, Halle MA, Decavallas O, Pichot C, Cros P. J Colloid Interface Sci 1998;202:251–260.
42. Carré A, Lacarrière V, Birch W. J Colloid Interface Sci 2003;260:49–55. [PubMed: 12742033]
43. Vairavapandian D, Vichchulada P, Lay MD. Anal Chim Acta 2008;626:119–129. [PubMed: 18790113]
44. Martin W, Zhu W, Krilov G. J Phys Chem B 2008;112:16076–16089. [PubMed: 19367836]
45. Johnson RR, Johnson AT, Klein ML. Nano Lett 2008;8:69–75. [PubMed: 18069867]
46. Diogo MM, Queiroz JA, Prazeres DM. J Chromatogr A 2002;944:119–128. [PubMed: 11833544]
47. Sigel H. Pure Appl Chem 2004;76:1869–1886.
48. Sushko ML, Shluger AL, Rivetti C. Langmuir 2006;22:7678–7688. [PubMed: 16922550]
49. Bezanilla M, Manne S, Laney DE, Lyubchenko YL, Hansma HG. Langmuir 1995;11:655–659.
50. Pastré D, Piétrement O, Fusil P, Landousy F, Jeusset J, David MO, Hamon L, Le Cam E, Zozime A. Biophys J 2003;85:2507–2518. [PubMed: 14507713]
51. Zheng J, Li Z, Wu A, Zhou H. Biophys Chem 2003;104:37–43. [PubMed: 12834825]

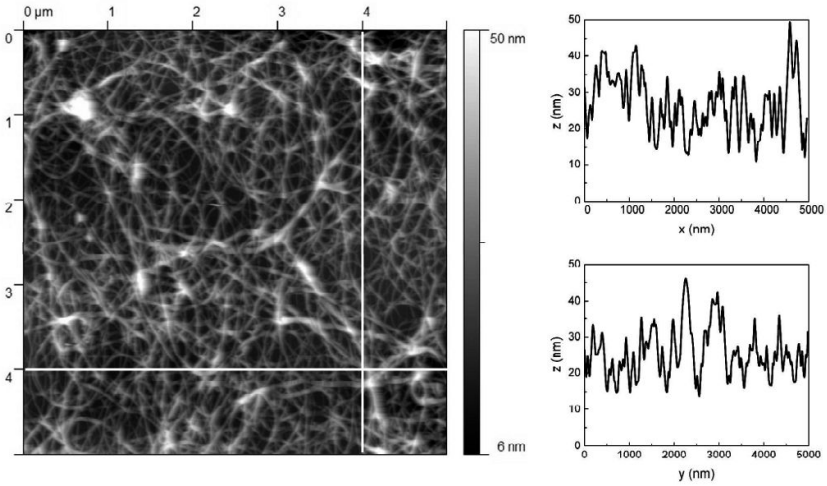

Figure 1.
AFM image and profiles recorded for the Si/SiO_2/CNT sorbent surface in aqueous solution.

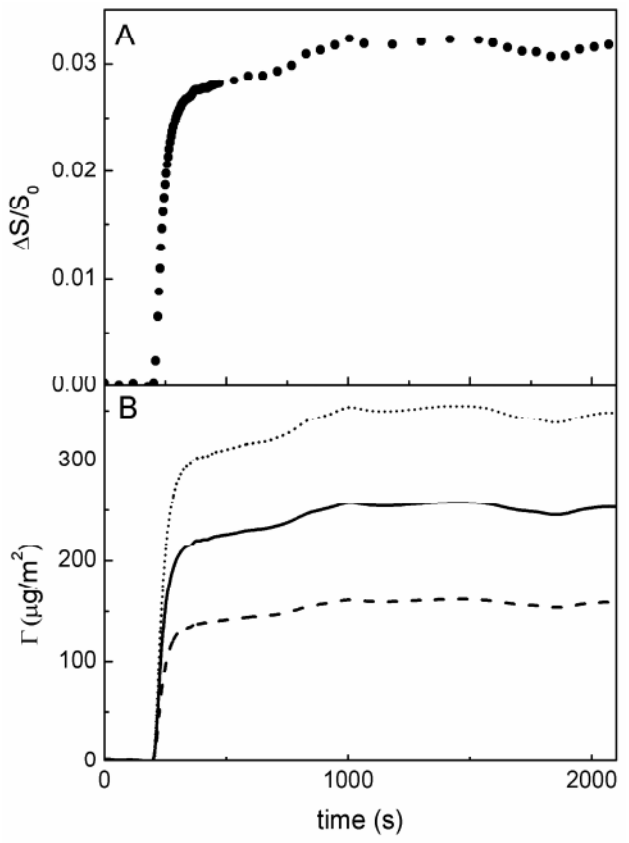

Figure 2.

(**A**) Change in the reflectometer signal ($\Delta S/S_0$) and (**B**) in the adsorbed amount (Γ) as a function of time during the adsorption–desorption process of 13 μg mL^{-1} $polyC_{20}$ on Si/SiO_2/CNT in PB + 100 mM NaCl pH 7. Γ was calculated from the average Q-factor (solid line), the average plus the standard deviation (dotted line) and the average minus the standard deviation (dashed line) originated from the CNT thickness standard deviation (35 ± 13 nm).

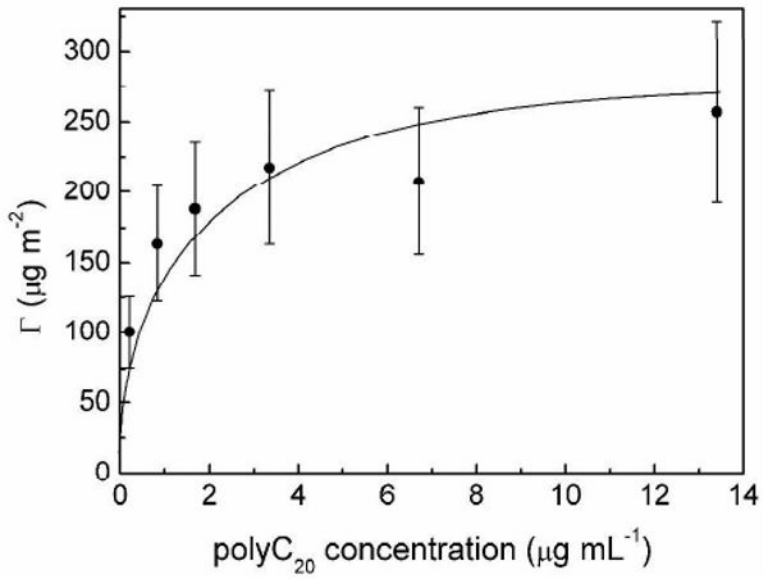

Figure 3.

Adsorption isotherm of $polyC_{20}$ adsorbed on Si/SiO_2/CNT in PB + 100 mM NaCl pH 7. The error bars are calculated from the standard deviation given by independent measurements and the line is only a guide to the eye.

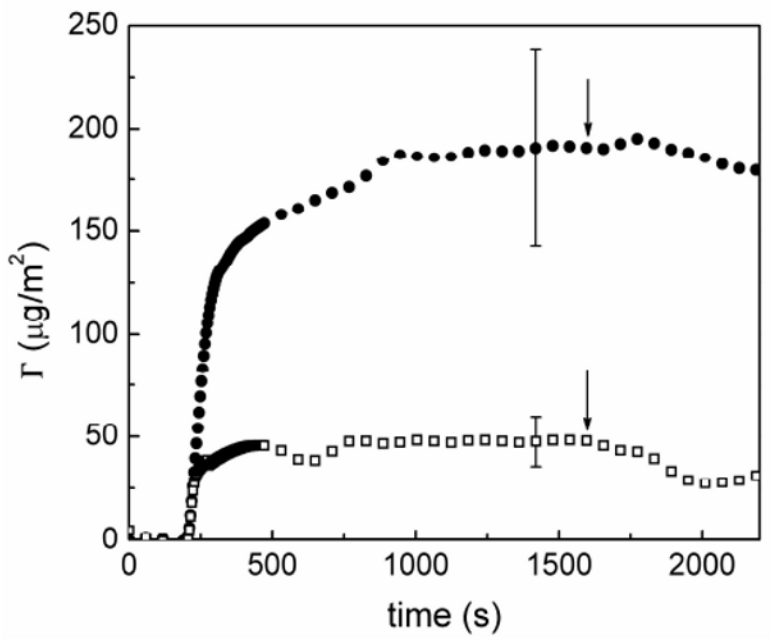

Figure 4.

Adsorption–desorption kinetics of 7 μg mL^{-1} $polyC_{20}$ (solid circles) and 8 μg mL^{-1} $polyT_{20}$ (open squares) on Si/SiO_2/CNT in PB + 100 mM NaCl (IS = 0.11) pH 7. Desorption was induced by adding a PB + 100 mM NaCl pH 7 (indicated by arrows). The error bars are calculated from the standard deviation given by independent measurements.

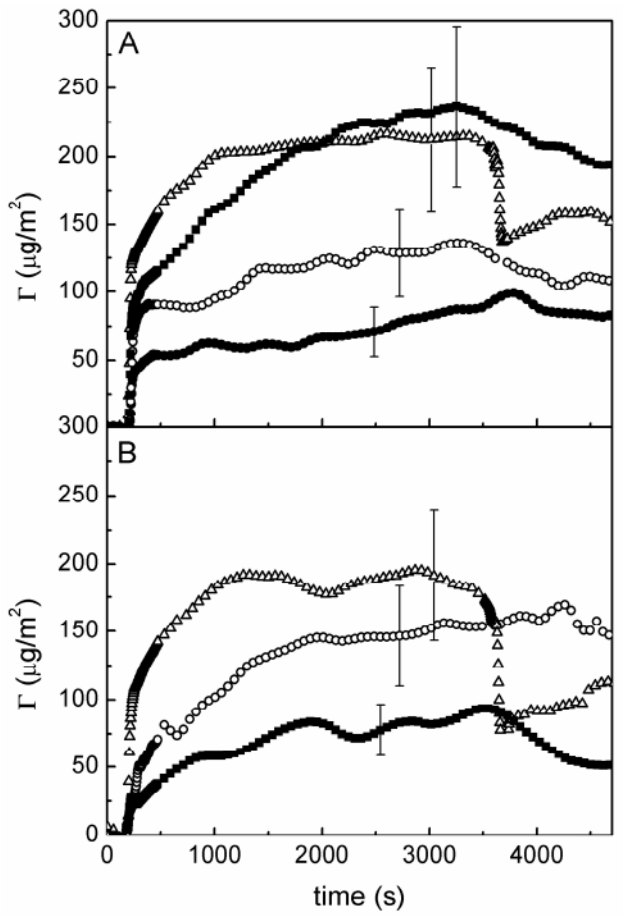

Figure 5.

Adsorption–desorption kinetics of 8 μg mL^{-1} $polyT_{20}$ on (**A**) Si/SiO_2/CNT and (**B**) Si/SiO_2 at pH 7 and two ionic strength: 0.11 (solid symbols), PB + 100 mM NaCl + 10 mM $MgCl_2$ (circles) and PB + 33 mM $MgCl_2$ (squares); 0.22 (open symbols), PB + 230 mM NaCl (triangles) and PB + 100 mM NaCl + 43 mM $MgCl_2$ (circles). Desorption was induced by adding the corresponding buffer solution. The error bars are calculated from the standard deviation given by independent measurements.

Table 1

Initial adsorption rates (v_i), saturation adsorbed amounts (Γ_{sat}) and desorbed percentages of 8 μg mL^{-1} $polyT_{20}$ at two ionic strength (IS). The standard deviation is given by independent measurements.

		Si/SiO_2/CNT			Si/SiO_2		
IS	**PB**	**v_i μg m^{-2} s^{-1}**	**Γ_{sat} μg m^{-2}**	**Desorbed %**	**v_i μg m^{-2} s^{-1}**	**Γ_{sat} μg m^{-2}**	**Desorbed %**
0.11	+ 100 mM [Na^+]	1.6 ± 0.4	50 ± 10	30	X	X	X
	+ 100 mM [Na^+] +10 mM [Mg^{2+}]	1.8 ± 0.5	60 ± 15	10	X	X	X
	+ 33 mM [Mg^{2+}]	4 ± 1	230 ± 60	15	1.3 ± 0.3	70 ± 20	40
0.22	+ 230 mM [Na^+]	6 ± 2	210 ± 50	30	7 ± 2	170 ± 40	35
	+ 100 mM [Na^+] + 43 mM [Mg^{2+}]	2.3 ± 0.6	90 ± 20	15	1.7 ± 0.4	120 ± 30	10

J Phys Chem C Nanomater Interfaces. Author manuscript; available in PMC 2011 March 18.